



**HAL**  
open science

## Over-coordination and order in hydrogenated nanostructured silicon thin films: their influence on strain and electronic properties

S. Vignoli, P. Mélinon, B. Masenelli, Pere Roca I Cabarrocas, A.M. Flank, Christophe Longeaud

### ► To cite this version:

S. Vignoli, P. Mélinon, B. Masenelli, Pere Roca I Cabarrocas, A.M. Flank, et al.. Over-coordination and order in hydrogenated nanostructured silicon thin films: their influence on strain and electronic properties. *Journal of Physics: Condensed Matter*, 2005, 17, pp.1279-1288. 10.1088/0953-8984/17/8/006 . hal-00321238

**HAL Id: hal-00321238**

**<https://centralesupelec.hal.science/hal-00321238>**

Submitted on 22 Feb 2022

**HAL** is a multi-disciplinary open access archive for the deposit and dissemination of scientific research documents, whether they are published or not. The documents may come from teaching and research institutions in France or abroad, or from public or private research centers.

L'archive ouverte pluridisciplinaire **HAL**, est destinée au dépôt et à la diffusion de documents scientifiques de niveau recherche, publiés ou non, émanant des établissements d'enseignement et de recherche français ou étrangers, des laboratoires publics ou privés.



Distributed under a Creative Commons Attribution - NonCommercial 4.0 International License

# Over-coordination and order in hydrogenated nanostructured silicon thin films: their influence on strain and electronic properties

S Vignoli<sup>1,5</sup>, P Mélinon<sup>1</sup>, B Masenelli<sup>1</sup>, P Roca i Cabarrocas<sup>2</sup>, A M Flank<sup>3</sup> and C Longeaud<sup>4</sup>

<sup>1</sup> Laboratoire de Physique de la Matière Condensée et Nanostructures (UMR 5586 CNRS), Université Claude Bernard, Bâtiment L Brillouin, La Doua, 69622 Villeurbanne cedex, France

<sup>2</sup> Laboratoire de Physique des Interfaces et des Couches Minces (UMR 7647 CNRS), Ecole Polytechnique, Route de Saclay, 91128 Palaiseau cedex, France

<sup>3</sup> Laboratoire LURE (UMR 130 CNRS), Université Paris Sud, Bâtiment 209D, BP34, 91898 Orsay cedex, France

<sup>4</sup> Laboratoire de Génie Electrique de Paris (UMR 8507 CNRS), Supélec, Université Paris VI et XI, 11 rue Joliot Curie, Plateau de Moulon, 91192 Gif sur Yvette cedex, France

E-mail: svignoli@lpmcn.univ-lyon1.fr

## Abstract

A set of hydrogenated nanostructured silicon films consisting of Si nanoparticles with a dense phase embedded in an amorphous matrix are analysed by means of several spectroscopic tools. Medium and short range order are determined by Raman spectroscopy and the average coordination versus the hydrogen content is measured from x-ray absorption spectroscopy. The improvement of transport properties such as the normalized photoconductivity with respect to that of hydrogenated amorphous silicon is explained by an inhomogeneous distribution of constraints in the samples. Our results on the order at different scales agree well with the paracrystalline model and suggest a well relaxed host matrix.

## 1. Introduction

Recently there has been new interest in hydrogenated polymorphous silicon (pm-Si:H) over amorphous hydrogenated silicon (a-Si:H). This is due to its advantages for applications such as low defect (dangling bond) densities before and after light degradation and enhanced transport properties [1–3] useful for applications. For example, its hole carrier mobility is ten times that of a-Si:H [4] while a large increase in the normalized photoconductivity  $\eta\mu\tau$  is also reported [1]. However, the exact structure remains elusive. This is an important issue since recent works point out that better ordered films should exhibit a low defect density after light degradation [5].

<sup>5</sup> Author to whom any correspondence should be addressed.

pm-Si:H phases can be viewed as small grains distorted by strain and embedded in a disordered matrix. Classical continuous random network (CRN) models, used for a-Si and based on the bond-switching algorithm of Wooten *et al* [6] integrate a collection of parameters such as the film density, the average coordination number, the bond length  $r$  and its distribution spread  $\Delta r$  and the bond angle  $\theta$  with its distribution spread  $\Delta\theta$ . For pm-Si:H silicon, earlier measurements done by high resolution transmission electron microscopy (HRTEM) reveal the presence of nanocrystallites in diamond phase and/or in metastable phases as reported for Si bulk in the high pressure region of the phase diagram [7, 8]. Recently, fluctuation electron microscopy experiments have also shown the signature of medium range order (MRO) on a length scale of the order of 1 nm due to the presence of nanoparticles, called paracrystallites [9]. A paracrystalline film consists in small grains which topologically have crystalline bonding but within which the atoms are significantly displaced from their crystalline lattice positions by strain caused by the grain boundaries. However, cluster inclusion involves further parameters such as the contribution of grain size, density, shape, crystallographic structure, spatial distribution and orientation. Besides, the concentration of bonded and molecular hydrogen must also be taken into account. Consequently, the heterogeneous nature of the material rules out a microscopic description from a molecular dynamics quench or numerical methods for generating the CRN models. An appropriate computer model must include the incorporation of crystallites (clusters) in the amorphous matrix which are not allowed to dissolve [10]. Such a procedure should forbid the host matrix relaxation near the cluster interface and leads to a metastable structure. Moreover, these classical models do not take into account the hydrogen content at the cluster–host matrix interface though hydrogen bonding certainly plays a prominent role in the cluster structure. For the hydrogen-free Si nanoclusters, with sizes less than a few nanometres, surface reconstruction is needed for stabilizing dangling bonds [11]. For the smallest ones, structures are close to stuffed fullerenes [12–14] and characterized by a spherical shape and over-coordinated atoms. Conversely, unreconstructed surfaces are predicted for Si clusters capped by hydrogen. The apparent paradox is that the very good transport properties observed in pm-Si:H films seem incompatible with the heterogeneous structure of the material.

In this paper we present a series of measurements on a set of Si:H compounds prepared by rf glow discharge in a PECVD reactor. We highlight the presence of nanosized dense phases in pm-Si:H films leading to an increase of the medium range order compared to conventional a-Si:H. In this perspective we explain the improved transport properties reported as well as the sensitivity to metastability.

## 2. Experimental details

pm-Si:H films have been deposited using a high hydrogen dilution (98%) of silane and rf power ( $90 \text{ mW cm}^{-2}$ ). Different structures, from the onset of the microcrystalline phase up to amorphous-like films, have been obtained by tuning the total pressure inside the reactor and keeping the substrate temperature at 423 K (see table 1). For comparison two a-Si:H films have been deposited at 423 and 523 K using pure silane and low pressure and rf power. More details are published elsewhere [3]. EXAFS spectroscopy has been performed on the SA-32 beam line of the SuperACO synchrotron facility in Orsay (France). We just recall here that EXAFS spectroscopy is the most powerful tool to probe *directly* the local environment around the absorbing species (first shell coordination and first neighbours distance). Si–K edge absorption spectra have been recorded collecting the total and/or the fluorescence emission at the photon energy [15]. Calibration has been done by comparison with a Si wafer. Average coordination number ( $n_{\text{exp}}$ ) and bond length ( $r$ ) have been deduced from the pseudo radial

**Table 1.** Deposition total pressure and parameters extracted from EXAFS, Raman and FTIR spectra for the studied films.  $\langle n_{\text{exp}} \rangle$  is the mean coordination number (error values being 0.07 for all films),  $\langle r \rangle$  and  $\Delta\theta$  are the bond length and bond angle distribution spread, respectively, and  $C_{\text{H}}$  is the bonded hydrogen content.

Sample	Label	$P$ (Pa)	$C_{\text{H}}$ (%)	$\langle n_{\text{exp}} \rangle$	$\langle r \rangle$ (Å)	$\Delta\theta$ (deg)
Si-2	ref	—	—	4	2.35	0
a-Si:H (423 K)		5	15.1	3.61	2.37(4)	9.2
a-Si:H (523 K)		5	12	3.71	2.37(0)	8.7
pm-Si:H	1	160	24.1	3.44	2.37(4)	7.7
pm-Si:H		186	20.4	3.71	2.36(7)	7.6
pm-Si:H		213	19.3	3.77	2.37(7)	7.8
pm-Si:H	3	239	19.0	3.73	2.35(4)	7.0
pm-Si:H		266	17.8	3.70	2.35(4)	7.5
pm-Si:H	2	292	16.1	3.59	2.35(4)	7.3

distribution functions (prdf) extracted from EXAFS spectra. Bond angle distribution spread  $\Delta\theta$  is estimated from first order Raman spectra (Raman DILOR XY operating at 514.5 nm) by fitting the high frequency part of the TO mode [16]. We note that the difference in the values of  $\Delta\theta$  are not sufficiently large to be examined by EXAFS. The bonded hydrogen content has been determined by Fourier transform infra-red (FTIR) spectroscopy using the procedure of Maley [17]. We would like to point out that the hydrogen content is accurate to  $\pm 2\%$  as shown by recent works [18]. For electrical measurements, coplanar chromium electrodes have been evaporated onto the films deposited on Corning glass substrates. The Urbach slope  $E_{\text{u}}$  was obtained by the constant photocurrent method whereas the photoconductivity was determined at 300 K using monochromatic light ( $\lambda = 650$  nm) and a flux of  $1.5 \times 10^{14} \text{ cm}^{-2} \text{ s}^{-1}$ .

### 3. Results and discussion

#### 3.1. Over-coordination and order in pm-Si:H

Figure 1 displays the pseudo radial distribution functions deduced from EXAFS spectroscopy for a set of samples. All the samples have the same features, in particular the lack of the second shell peak at  $3.4 \text{ \AA}^{-1}$  corresponding to second neighbour distance. This indicates a short range order without large crystallized regions ( $> 2$  nm). It agrees with Raman spectra where no band is observed near  $520 \text{ cm}^{-1}$  (see below). The careful analysis of the first shell peak gives the mean average coordination number summarized in table 1. Figure 2 displays the average coordination number  $\langle n_{\text{exp}} \rangle$  versus the bonded hydrogen content  $C_{\text{H}}$ . The two pm-Si:H films deposited at the edges of the pressure range, namely 160 and 292 Pa (labelled ‘1’ and ‘2’, respectively), as well as the a-Si:H ones, agree well with the theoretical curve (solid curve) assuming a ‘perfect’ CRN model ( $\langle n_{\text{CRN}} \rangle = \langle n_{\text{a-Si}} \rangle - C_{\text{H}}/(1 - C_{\text{H}})$ ) and an average coordination number for hydrogen free amorphous silicon of 3.8 [19]. Earlier works have shown that films deposited at 160 Pa have a structure at the onset of microcrystallinity (diamond-like nanocrystallites have been observed by HRTEM [8] and we point out that high hydrogen content is usually found for films deposited in this regime [20] as shown in table 1); whereas films deposited at high pressures appear amorphous-like [4]. Thus, no departure from the theoretical curve is expected for these films. The striking result is the mismatch between the other pm-Si:H samples and the theoretical curve. This shows that clusters embedded into the host matrix are over-coordinated. Assuming a single cluster size and a single phase, the volume fraction of over-coordinated atoms is  $x = (\langle n_{\text{exp}} \rangle - \langle n_{\text{CRN}} \rangle) / (\langle n_{\text{cl}} \rangle - \langle n_{\text{CRN}} \rangle)$ ,  $\langle n_{\text{cl}} \rangle$

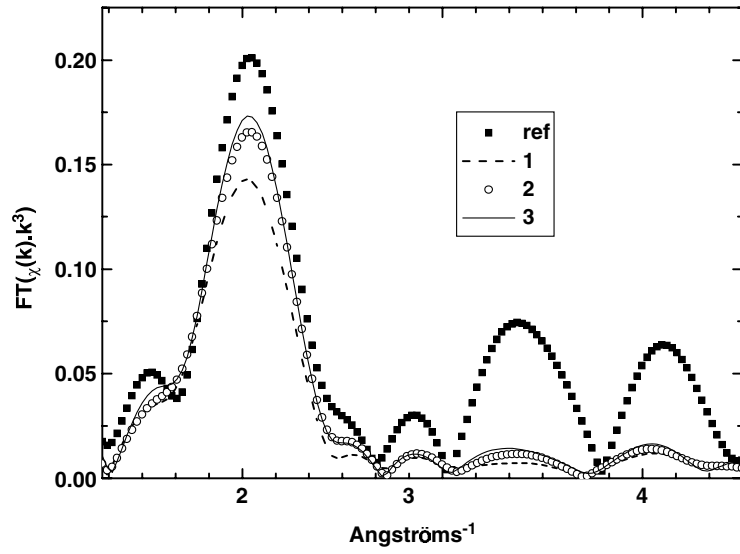


**Figure 1.** Fourier transforms  $k^3\chi(k)$  at 300 K for the samples labelled 1–3 (see table 1). The diamond phase is given as a reference. The coordination number is calculated by comparison between a sample and the reference together. Simulation is done within the FEFF-FIT program.

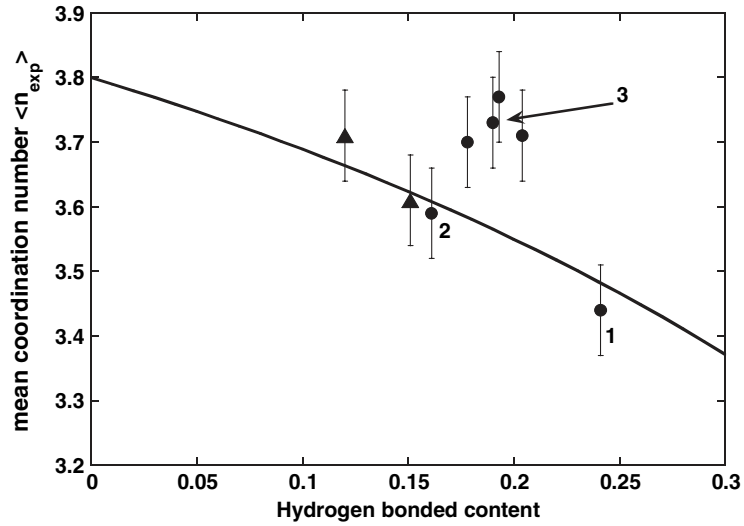


**Figure 2.** Mean coordination number versus the hydrogen content. The numbers correspond to the labels indicated in table 1. ( $\blacktriangle$ ) a-Si:H films and ( $\bullet$ ) pm-Si:H films. The solid curve is the theoretical curve assuming a perfect CRN model. Hydrogen content  $C_H$  is deduced from infra-red spectroscopy.

being the average coordination of the Si atoms inside a cluster. Since the prdf are close to those observed in a-Si, we deduce that the host lattice is mainly formed by tetrahedrally coordinated atoms. In the case of embedded clusters, we can expect that the concentration  $x$  is far from the percolation threshold ( $x < 20\%$ ) to ensure isolated clusters. If percolation threshold was reached the films will have a metallic-like character which is not observed by

electrical measurements [1]. An estimation of the cluster density requires the knowledge of the mean cluster size  $N_c$ . Further information is given by the density of the films  $\langle d_{\text{exp}} \rangle$  since  $x = (\langle d_{\text{exp}} \rangle - \langle d_{\text{CRN}} \rangle) / (\langle d_{\text{cl}} \rangle - \langle d_{\text{CRN}} \rangle)$ ,  $\langle d_{\text{CRN}} \rangle$  and  $\langle d_{\text{cl}} \rangle$  being the density of the CRN and the cluster, respectively. Both equations give independent values for  $x$ . Assuming embedded clusters belonging to a dense phase such as  $\beta$ -tin Si ( $\langle n_{\text{cl}} \rangle = 6$ ,  $\langle d_{\text{cl}} \rangle = 3.28$ ), the fraction  $x$  for a typical sample (labelled '3' in table 1) is 7% from density measurements [21] and 8.5% from EXAFS, corroborating a distribution of isolated clusters. The choice of  $\beta$ -tin is still arbitrary but coincides with the first observed dense phase when applying pressure onto the Si diamond phase. Relaxation may induce the classical  $\beta$ -tin  $\rightarrow$  BC-8 or ST-12 transition but would not change the physics of the following discussion. To discuss the possible structures of the clusters in our films, we consider three cases.

In the first case, clusters have a core shell structure with an outer shell of molecular hydrogen. This is equivalent to a free cluster without noticeable interaction with the host matrix. Surface reconstruction appears leading to the formation of pentagonal rings [22]. The increase of the coordination number only appears for the smallest sizes. For example, the average coordination number  $\langle n_{\text{cl}} \rangle$  ranges between 3.6 and 4.2 following the Si<sub>33</sub> isomer (the size is less than 1 nm in diameter) [14]. This over-coordination is also reported in Si-cluster assembled films [14]. Since there is no significant interaction between embedded clusters and the host matrix, this case corresponds to the superposition of isolated clusters and a-Si with voids. However, we discard this scenario since the excess of coordination in such clusters is too low to meet the condition  $x < 20\%$ . In addition spectroscopic ellipsometry analyses [4] and mass density measurements [21] have shown that pm-Si:H films are free of microvoids.

In a second case, hydrogen atoms cap the cluster leading to unreconstructed surfaces (diamond phase). We also discard this hypothesis since the average coordination in this structure is too small to meet the experimental values since, in this case, the mean coordination number is 4 in the volume of the clusters and 2 or 3 at their surface. However we note that this kind of cluster likely exists in our films as evidenced by H bonding [3] and H evolution analyses [21]. Simulations performed by Pan and Biswas [23] have very recently confirmed these last results.

In the third case, clusters are hydrogen free. Neglecting pressure and temperature contributions, the interface between the clusters and the matrix is usually characterized by the excess of interfacial energy [24],  $A\sigma_{\text{ac}} = E - N_c\varepsilon_c - N_a\varepsilon_a$ ,  $E$  being the total cohesive energy of a sample with an interface of area  $A$ ,  $N_{c,a}$  the number of atoms,  $\varepsilon_{c,a}$  the cohesive energy per atom, with subscripts c, a standing for crystal and amorphous phases, respectively. For large clusters with diamond phase,  $\sigma_{\text{ac}} = 0.48$  eV with  $\varepsilon_c - \varepsilon_a = 0.12$  eV [25]. The interface between crystal and amorphous phases has a thickness of about 0.7 nm [24]. For small clusters with dense phases, the excess interfacial energy is not a reliable parameter since the thickness of the interface is of the same order of magnitude as the cluster radius ( $< 1$  nm). As a consequence it is meaningful to estimate  $N_{c,a}$ . The most striking effect is the difference  $\varepsilon_c - \varepsilon_a$  which is *always negative* since all the dense phases are less stable than diamond and amorphous phases [25]. This emphasizes the high metastability and corroborates the large stress observed [3]. According to the Si phase diagram, the minimum pressure to observe a dense phase for Si is about 12 GPa ( $\beta$ -tin transition) [25]. This pressure is needed to maintain the dense phase inside the cluster. It is much greater than the measured average stress in our films,  $P_{\text{exp}} = 0.8$  GPa [3]. However, the latter is much greater than those observed in a-Si:H,  $P_{\text{exp}} = 0.15 - 0.3$  GPa [20]. This leads one to consider a model with a distribution of the constraint field around the clusters. It agrees with the formation of micro cracks in the pm-Si:H films under external mechanical stress, as we have observed. The large stress at the interface is due to the rehybridization of Si bonds ( $\beta$ -tin has a metal-like character) and the large

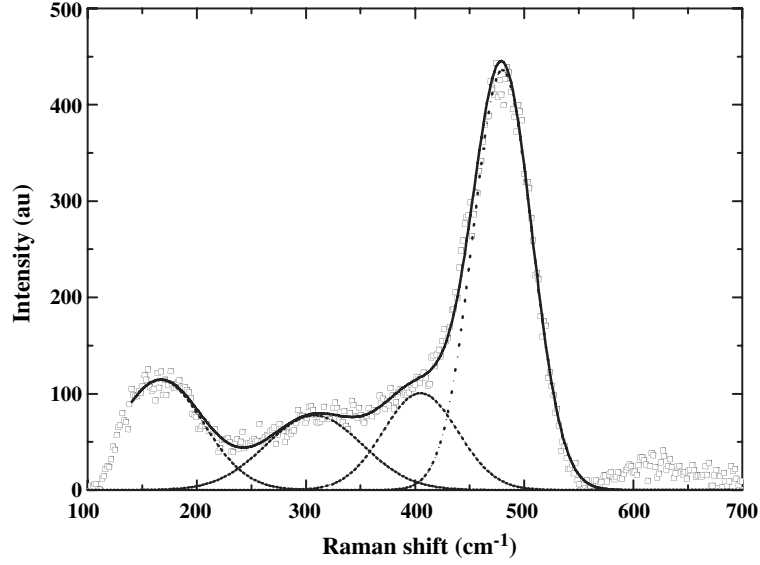


**Figure 3.** First order Raman spectrum for a pm-Si:H film deposited at 213 Pa ( $\square$ ). The solid curve is the sum of the different modes obtained by deconvolution and represented by the different dotted curves (see the text).

difference between the bond length in the matrix and in the clusters ( $\langle r \rangle = 0.237$  nm in a-Si:H and  $\langle r \rangle = 0.248$  nm in  $\beta$ -tin, respectively). The stress inside the cluster is zero since we expect a full relaxation. The stress given by an average fraction  $\langle x' \rangle$  at the interface is  $P_{tr} = 12$  GPa. Only a fraction  $x'$  of matrix atoms, standing at the shells surrounding the clusters, generates the interface pressure  $P_{tr} = 12$  GPa needed to stabilize the high density clusters. The stress  $P_{pm-Si:H}$  in the host lattice far from the clusters is given by  $P_{pm-Si:H} = (P_{exp} - x'P_{tr})/(1 - x - x')$ . This stress vanishes for  $x' > 0.07$ . Since HRTEM observations [26] reveal that the host lattice is fully relaxed, we assume  $x' = 0.07$  in the following. Furthermore,  $x'$  is connected to  $N_c$  through the geometric relation  $x' = (x/12.2)N_c^{0.5}$  leading to  $N_c = 100$  atoms (1.5 nm diameter). Thus, the name polymorphous for this kind of material is well justified since different crystalline structures are likely present in our films, say diamond like structures for the nanoparticles passivated by hydrogen and with radius larger than 2 nm and dense metastable structures with radius smaller than 2 nm otherwise. Diamond and metastable structures as well as their size have been revealed by HRTEM micrographs in [8] and [7], respectively. Moreover we would like to point out that pm-Si:H films grow homogeneously. In particular, no columnar structures have been observed by cross sectional HRTEM studies [26] (except for some epitaxial growth at the early stage of deposition on silicon substrates). This is confirmed by the absence of microvoids [4] since a columnar growth is always accompanied by microvoids.

Following the theoretical works on the paracrystalline films, the embedded clusters should have a beneficial effect on the MRO. Raman spectroscopy can help to study the MRO since paracrystallites in a host matrix have demonstrated changes in the vibrational density of states [27]. Indeed Gerbi *et al* [28] have recently shown that the intensity of the LO/TO peak ratio correlates with MRO and therefore may provide a very convenient tool for evaluating MRO. Figure 3 shows a Raman spectrum in the range  $100 \text{ cm}^{-1}/1000 \text{ cm}^{-1}$  and the different Gaussian-like bands after deconvolution. A remark is necessary at this stage. We can observe in figure 3 that the TA mode is not fully resolved due to the cut-off of the spectrometer at

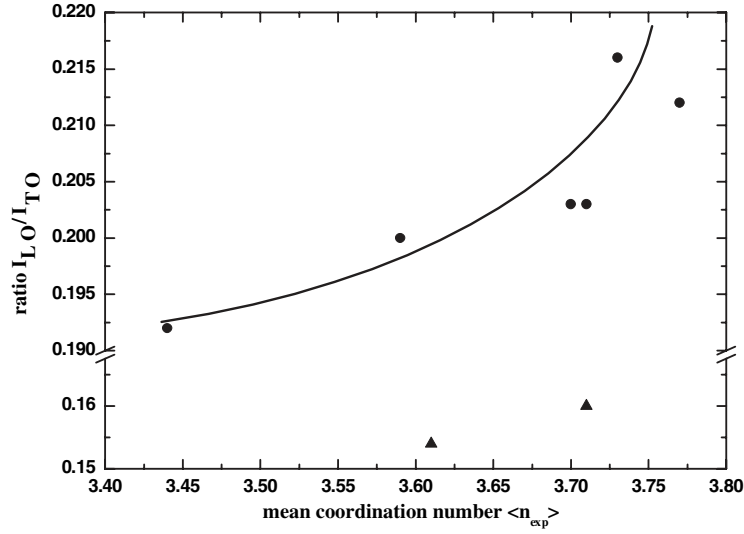


**Figure 4.** Ratio of the intensity of the longitudinal optical mode with the transverse optical mode ( $I_{\text{LO}}/I_{\text{TO}}$ ) versus the mean coordination number ( $n_{\text{exp}}$ ) for ( $\blacktriangle$ ) a-Si:H films and ( $\bullet$ ) pm-Si:H films. The solid curve is a guide to the eye.

$\sim 100 \text{ cm}^{-1}$  and thus the spectra above  $\sim 150 \text{ cm}^{-1}$  were rigorously fitted with four Gaussians corresponding to the TA mode at  $\sim 150 \text{ cm}^{-1}$  (only the high frequency part of this mode is fitted due to the cut-off of our spectrometer), the LA mode at  $\sim 310 \text{ cm}^{-1}$ , the LO mode at  $\sim 410 \text{ cm}^{-1}$  and the TO mode at  $\sim 480 \text{ cm}^{-1}$ . The procedure was as follow: we first fitted the high frequency part of the TO and TA modes with Gaussian functions and then the contribution of the entire TO and TA modes was subtracted from the whole spectra before fitting the longitudinal (LA and LO) modes. In figure 4 we have plotted the LO/TO peak ratios versus the mean coordination number for our pm-Si:H films. The increase of the LO/TO peak ratio with  $\langle n_{\text{exp}} \rangle$  clearly indicates that the MRO is increased when adding nanosized ordered objects in the matrix and thus confirming the theoretical results of Voyles *et al* [27]. As expected the LO/TO peak ratio is lower for our a-Si:H films than the ones found in pm-Si:H (see figure 4). From Raman spectroscopy we can also check the short range order (SRO) by means of the bond angle distribution spread  $\Delta\theta$  deduced from the FWHM of the TO mode using the empirical relation of Beeman *et al* [29]. No clear correlation has been found between  $\Delta\theta$  and the mean coordination number. This result is not surprising at all since the grain boundaries are highly distorted by strain and thus large bond angle distortions are expected. Indeed Biswas and Pan [30] have reported such large bond angle distribution exceeding  $15^\circ$  in the grain boundary whose width is of the order of 1 nm. However the values of  $\Delta\theta$  reported in table 1 are lower for the pm-Si:H films than the ones for our a-Si:H samples. That is to say that  $\Delta\theta$  is lower for films with cluster inclusions than for homogeneous a-Si:H films despite the high degree of disorder at the grain boundary for mixed-phase films. Our results concerning MRO and SRO are in full agreement with the results of Biswas and Pan [30] who found a beneficial ordering of the amorphous matrix in the presence of crystallites by molecular dynamics, and with the results of Fontcuberta i Morral *et al* [26] who highlighted the increased ordering of the matrix by TEM image analyses. Finally, we like to point out that such low values of  $\Delta\theta$  found for our pm-Si:H films can only be explained by introducing ordered objects in the amorphous matrix [31].

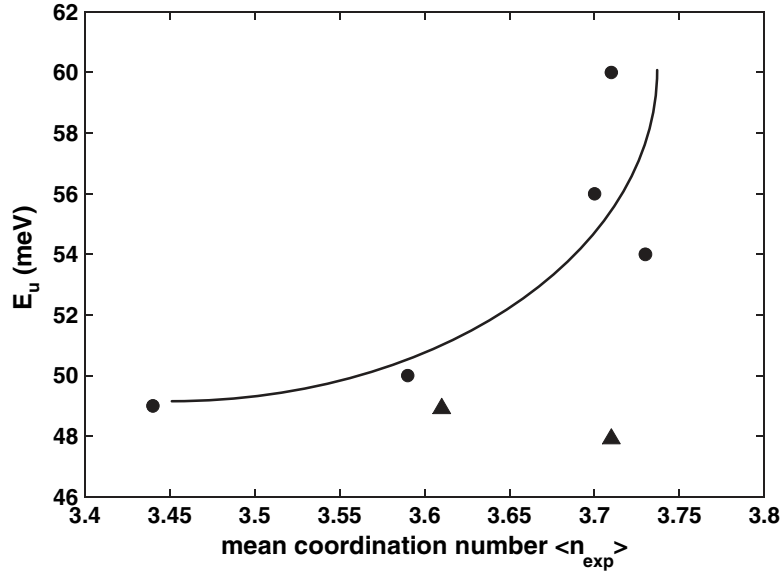


**Figure 5.** Urbach slope ( $E_u$ ) versus the mean coordination number ( $n_{\text{exp}}$ ) for (▲) a-Si:H films and (●) pm-Si:H films. The solid curve is a guide to the eye.

### 3.2. Links with electronic and metastable properties

The Urbach slope  $E_u$ , which quantifies the density of states in the valence band tail is, within a constant, a good measure of the average strain energy per network bond [32]. For purely amorphous films, the higher  $E_u$  the more disordered is the film. However, the situation is quite different for mixed phase material and, for example, a large increase of  $E_u$  is observed in microcrystalline silicon [33]. This increase is believed to be due to an increase of the strain energy per network bond at grain boundaries [32]. Figure 5 shows that  $E_u$  increases with the mean coordination number for our pm-Si:H films. This result confirms that grain boundaries are electrically active, as was anticipated by molecular dynamics calculations performed on paracrystalline films [10]. Keeping in mind that valence band tail states are due to strained (shortened) bonds [34], the increase of  $E_u$  with the mean coordination number is thus self-explained since the large compressive stress at grain boundaries will shorten the bonds.

Moreover, as recently shown in amorphous diamond-like carbon films, medium range ordering may play an important role in stress relaxation [35] and thus in transport properties. This is illustrated by the normalized photoconductivity  $\eta\mu\tau$  versus the mean coordination number behaviour. Figure 6 displays an exponential relationship between  $\eta\mu\tau$  and  $\langle n_{\text{exp}} \rangle$ . This relationship would be rather amazing if we were considering a homogeneous sample. However, we must keep in mind that the increase in the average coordination number only appears for isolated regions with compact phases. The increase in  $\eta\mu\tau$  is understood as constraints are released in the host matrix leading to low defect densities [1] and electron capture cross sections [36]. The lowering of the electron capture cross section with the release of the constraints in the matrix is consistent with the model developed by Kounavis and Mytilineou [37].

Nevertheless, the metastability induced by the excess of constraints near the clusters is well observed by the evolution of  $\eta\mu\tau$  after light degradation (figure 6). The decrease of the slope clearly indicates that pm-Si:H samples undergo a relaxation of the constraints near the clusters

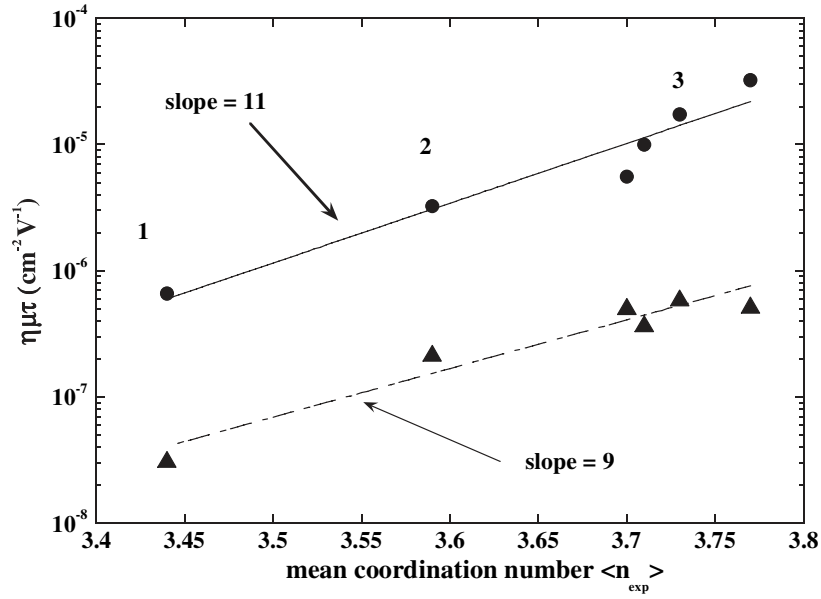


**Figure 6.** Normalized photoconductivity ( $\eta\mu\tau$ ) versus the mean coordination number for our pm-Si:H films. The numbers correspond to the labels indicated in table 1. (●) as-deposited state (▲) light-soaked state.

since new defects appear preferentially in highly distorted regions (i.e. at the interface) [5]. We can thus expect an increase in the defect creation rate as observed [2] and predicted by recent models invoking over-coordinated defects (floating bonds) [5]. The release of strain in the interfacial region may lead to the disappearance of these highly metastable phases. This would lead first to volume expansion after light degradation (which is enhanced in mixed-phase material) [38], second to irreversible phenomena after light-degradation/annealing cycles [39] and third to a decrease of the MRO upon light degradation [40]. Finally, we point out that p-bonding states of the top of the valence band are more sensitive to the angular disorder than s-like states. The low bond angle distribution in pm-Si:H films (see table 1) is consistent with the increase in hole mobility [4].

#### 4. Conclusion

In conclusion, we have reported on the excess of coordination as well as an increase of the medium range order in pm-Si:H films as compared to a-Si:H. All the features deduced from several spectroscopic tools suggest a large and critical metastability of such samples. The improvement of the normalized photoconductivity  $\eta\mu\tau$  is explained by the introduction of a distribution field for the constraints. The stress is maximum near the cluster interface and probably close to zero far away. This metastability is a challenge for theoretical investigations since the total energy is probably far from those reported in a-Si:H samples. Our results agree well with the prediction from the paracrystalline model recently developed. It remains to elucidate the question of the microscopic mechanisms responsible for the formation of such highly metastable structures in PECVD reactors and in particular the role of hydrogen in the growth process. Finally, we would like to stress that more theoretical works are needed to relate the structural properties of such nanostructured films to their good transport properties.

## References

- [1] Meaudre M, Meaudre R, Butté R, Vignoli S, Longeaud C, Kleider J P and Roca i Cabarrocas P 1999 *J. Appl. Phys.* **86** 946
- [2] Butté R, Meaudre R, Meaudre M, Vignoli S, Longeaud C, Kleider J P and Roca i Cabarrocas P 1999 *Phil. Mag. B* **79** 1079
- [3] Vignoli S, Butté R, Meaudre R, Meaudre M and Brenier R 2003 *J. Phys.: Condens. Matter* **15** 7185
- [4] Fontcuberta i Morral A, Brenot R, Hamers E A G, Vanderhagen R and Roca i Cabarrocas P 2000 *J. Non-Cryst. Solids* **266–269** 48
- [5] Biswas R, Pan B C and Ye Y Y 2002 *Phys. Rev. Lett.* **88** 205502
- [6] Wooten F, Winer K and Weaire D 1985 *Phys. Rev. Lett.* **54** 1392
- [7] Viera G, Mikikian M, Bertran E, Roca i Cabarrocas P and Boufendi L 2002 *J. Appl. Phys.* **92** 4684
- [8] Butté R, Vignoli S, Meaudre M, Meaudre R, Marty O, Saviot L and Roca i Cabarrocas P 2000 *J. Non-Cryst. Solids* **266–269** 263
- [9] Treacy M M J, Gibson J M and Keblinski P J 1998 *J. Non-Cryst. Solids* **231** 99
- [10] Nakhmanson S M, Voyles P M, Mousseau N, Barkema G T and Drabold D A 2001 *Phys. Rev. B* **63** 235207
- [11] Puzder A, Williamson A J, Reboledo F A and Galli G 2003 *Phys. Rev. Lett.* **91** 157405
- [12] Kaxiras E 1990 *Phys. Rev. Lett.* **64** 551
- [13] Röthlisberger U, Andreoni W and Parinello M 1994 *Phys. Rev. Lett.* **72** 665
- [14] Mélinon P, Masenelli B, Perez A, Pellarin M and Broyer M 2002 *C. R. Physique* **3** 273
- [15] Belot V, Corriu R J P, Leclercq D, Lefèvre P, Mutin P H, Vioux A and Flank A M 1991 *J. Non-Cryst. Solids* **127** 207
- [16] Tourir H, Morhange J-F and Dixmier J 1999 *Solid State Commun.* **110** 315
- [17] Maley N 1992 *Phys. Rev. B* **46** 2078
- [18] Fontcuberta i Morral A, Roca i Cabarrocas P and Clerc C 2004 *Phys. Rev. B* **69** 125307
- [19] Glover C J, Foran G J and Ridgway M C 2003 *Nucl. Instrum. Methods Phys. Res. B* **199** 195
- [20] Kroll U, Meier J, Shah A, Mikhailov S and Weber J 1996 *J. Appl. Phys.* **80** 4971
- [21] Vignoli S, Fontcuberta i Morral A, Butté R, Meaudre R and Meaudre M 2002 *J. Non-Cryst. Solids* **299–302** 220
- [22] Pandey K C 1982 *Phys. Rev. Lett.* **49** 223
- [23] Pan B C and Biswas R 2004 *J. Non-Cryst. Solids* **333** 44
- [24] Bernstein N, Aziz M J and Kaxiras E 1998 *Phys. Rev. B* **58** 4579
- [25] Chelikowsky J R and Franciosi A (ed) 1991 *Electronic Materials (Springer Series in Solid-State Sciences vol 95)* (Berlin: Springer)
- [26] Fontcuberta i Morral A, Hofmeister H and Roca i Cabarrocas P 2002 *J. Non-Cryst. Solids* **299–302** 284
- [27] Voyles P M, Zotov N, Nakhmanson S M, Drabold D A, Gibson J M, Treacy M M J and Keblinski P 2001 *J. Appl. Phys.* **90** 4437
- [28] Gerbi J E, Voyles P M, Treacy M M J, Gibson J M and Abelson J R 2003 *Appl. Phys. Lett.* **82** 3665
- [29] Beeman D, Tsu R and Thorpe M F 1985 *Phys. Rev. B* **32** 874
- [30] Biswas R and Pan B C 2003 *Mater. Res. Soc. Symp. Proc.* **762** A11.4.1
- [31] Tsu D V, Chao B S, Ovshinsky S R, Jones S J, Yang J, Guha S and Tsu R 2001 *Phys. Rev. B* **63** 125338
- [32] Kaiser I, Nikel N H, Fuhs W and Pilz W 1998 *Phys. Rev. B* **58** R1718
- [33] Jun K H, Carius R and Stiebig H 2002 *Phys. Rev. B* **66** 115301
- [34] Fedders P A, Drabold D A and Nakhmanson S 1998 *Phys. Rev. B* **58** 15624
- [35] Chen X, Sullivan J P, Friedmann T A and Gibson J M 2004 *Appl. Phys. Lett.* **84** 2823
- [36] Meaudre R, Meaudre M, Butté R and Vignoli S 1999 *Phil. Mag. Lett.* **79** 763
- [37] Kounavis P and Mytilineou E 1995 *Solid State Phenom.* **44–46** 715
- [38] Stratakis E, Spanakis E, Tzanetakis P, Fritzsche H, Guha S and Yang J 2002 *Appl. Phys. Lett.* **80** 1734
- [39] Longeaud C, Roy D and Saadane O 2002 *Phys. Rev. B* **65** 085206
- [40] Gibson J M, Treacy M M J, Voyles P M, Jin H C and Abelson J R 1998 *Appl. Phys. Lett.* **73** 3093